Radio Propagation Characteristics in Underground Streets Crowded with Pedestrians

YOSHIO YAMAGUCHI, MEMBER, IEEE, TAKEO ABE, MEMBER, IEEE, AND TOSHIO SEKIGUCHI, FELLOW, IEEE

Abstract—**Radio propagation characteristics in an underground street crowded with pedestrians are presented. Measurements were carried out on vertical and horizontal polarization characteristics in a frequency range from 250 MHz to 12.4 GHz. In the analysis, the region with pedestrians is modeled as a lossy, homogeneous dielectric slab. Based on the method of effective dielectric constant, some numerical results are presented for the attenuation constant and for the field distribution in the cross section and are compared with experimental data. It is shown that the method is applicable in determining the propagation characteristics in underground streets crowded with pedestrians.**

Key Words—**Propagation, UHF, microwave, underground street, pedestrians, attenuation constant.**

Index Code—**J7e/f.**

I. Introduction

MANY theoretical analyses have been presented on the propagation characteristics in hollow tunnels [1]–[4], corridors in buildings [5], and underground streets [6] from the viewpoint of wireless communication systems, such as portable phones for emergency and disaster. However, only a few investigations [7], [8] have been presented on propagation characteristics that take into account the effect of obstacles, such as vehicles in the structures. This is because of the difficulty of treating obstacles in an analysis. In the actual environment, obstacles to radio propagation always exist, and radio communication must be carried out in the environment. Hence, it is necessary to investigate the propagation characteristics considering the effect of obstacles. On the other hand, experimental measurements, which have been carried out on vehicles in tunnels at UHF band [7], are still needed in higher frequencies and at various locations.

Underground streets crowded with pedestrians may be similar, in general, to tunnels crowded with vehicles. However, the environment for radio propagation is somewhat different from that of tunnels, because the obstacles or scatterers for radio propagation are not necessarily metallic bodies. There are so many scatterers—pillars, signboards, metallic plates, etc.—on irregular walls along the structure. There are also many people walking or strolling along the street. The environment also depends on the traffic density of pedestrians. The scattering loss and/or the absorption loss by these scatterers and pedestrians will become the dominant factor for attenuation in higher frequencies above the UHF band.

With the permission of an administrative office, we took measurements of radio propagation characteristics in an underground street crowded with pedestrians (its daily condition). The measurements were carried out in a frequency range from 250 MHz to 12.4 GHz and were performed for horizontally and vertically polarized waves. The field strength in regions with and without pedestrians along the structure and the field distribution in a transverse cross section were measured. As a result, the field strength received in the lower region with pedestrians was larger than that in the higher region above pedestrians in frequency bands below 5–6 GHz; i.e., the maximum field strength occurred in the region with pedestrians.

This paper extends the earlier work [6] and reports both the theoretical and experimental results on the propagation characteristics in an underground street crowded with pedestrians, to provide fundamental data for radio communications and for EMC problems.

In the analysis, the structure is modeled as a partially filled lossy waveguide, where the surrounding floor, ceiling, and sidewalls have different electrical properties; a region with pedestrians is modeled as a lossy homogeneous dielectric slab. The propagation constant for this modified structure is determined based on the method of effective dielectric constant. Then the attenuation constant and the field distribution are compared with experimental ones. It is shown that calculated results agree with the experimental results, and that the approach based on the method is applicable in determining the propagation characteristics in underground streets crowded with pedestrians.

II. Experiment

The underground street under test was Nishibori ROSA, located in Niigata-shi, Japan. The street is 330 m long, 3 m high, and 6.4 m wide. The detailed composition is shown in [6]. Outside the sidewalls there are many stores, which are open during the day, and there are many people walking and/or strolling over all regions with an average traffic density of about 2–3 persons/10 m.

A block diagram for the measuring apparatus is shown in Fig. 1. The transmitting and receiving antennas used are listed in Table I. A transmitting antenna was fixed at the center of the cross section and almost at one end of the underground street. A sweep oscillator (maximum output power 50 mW)

Manuscript received June 1, 1987. This work was supported in part by the Grant in Aid of the Education Ministry of Japan: Encouragement of Young Scientist (A) 61750295.

Y. Yamaguchi and T. Abe are with the Department of Information Engineering, Faculty of Engineering, Niigata University, Ikarashi 2-8050, Niigata 950-21, Japan. Tel. 025-262-7219.

T. Sekiguchi is with the National Tokyo Technical College, Hachiouji 1220-2, Tokyo 193, Japan. Tel. 0426-61-3066.

IEEE Log Number 8820085.

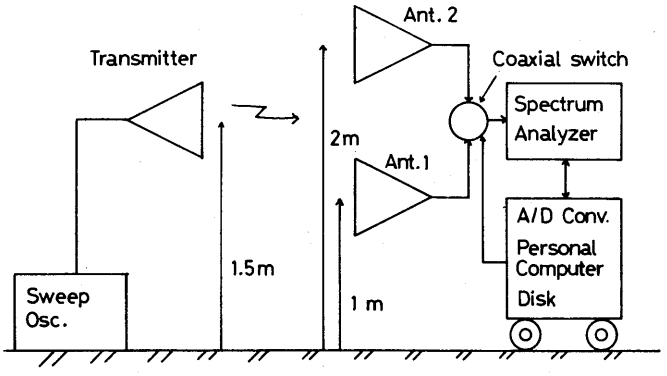

Fig. 1. Block diagram for the measuring apparatus.

TABLE I
ANTENNAS USED IN THE MEASUREMENT

Frequency band	Transmitting antenna	Receiving antenna
250-750 MHz	Yagi dipole array	Yagi dipole array
500-1500 MHz	Log-periodic dipole array	Log-periodic dipole array
1.4-12.4 GHz	Pyramidal horns	Pyramidal horns

was used as a signal source in order to obtain continuous frequency characteristics. We employed two antennas to receive the field strength at different heights, one at a height of 2 m from the floor and the other at a height of 1 m. These heights correspond to observing positions in the region (of upper free space) without pedestrians and in the region with pedestrians. A spectrum analyzer, used as a receiver, was connected to a personal computer, where the output field strength (continuous spectrum) was converted into digital signals and was recorded onto a mini-floppy disk. In the measurement, these receiving antennas were changed alternatively by a coaxial switch, controlled by the personal computer. We moved the receiving instrument along the centerline of the underground street at intervals of 1.1 m, corresponding to the interval of tiles on the floor. After we received the field strength at one point and recorded it onto the mini-floppy disk, we moved toward the next point 1.1 m away from the former and repeated the same operation until we finally came to a point where the field strength faded out and could not be picked up.

We measured the propagation characteristics on the same polarization (horizontal to horizontal, H–H, vertical to vertical, V–V) for all frequency ranges and on the orthogonal polarization (vertical to horizontal, or vice versa, V–H) at some frequency bands.

Preceding the propagation test, we measured the RF environment by the spectrum analyzer and confirmed that there was no ambient noise in the measurement frequency range. Hence, the received field strength was all due to the transmitter. Calibration of the measurement setup was not done because we could not measure the absolute electric field strength, including antenna gains, etc., by our instruments. However, the relative field strength in the region far from the transmitter is sufficient to determine the propagation characteristics; hence, we limit our analysis or discussion to the far region only.

III. Measurement Results

Fig. 2 shows some examples of received field strength along the underground street crowded with pedestrians. These values are relative ones, i.e., they correspond to the direct signal values of the spectrum analyzer; however, the relative values against distance from a transmitting antenna are sufficient to determine the propagation characteristics. Thus, the vertical axis in Fig. 2 is measured by 10 dB/div to show the same level of the spectrum analyzer.

Fluctuations are observed in almost all regions, independent of frequency. The value of fluctuation is up to 20 dB.

The straight lines drawn in Fig. 2 are the regression lines in the corresponding regions, with the gradients representing the attenuation constants. It is seen that the field strength received in the lower position (Antenna 1) is larger than that received in the higher one (Antenna 2). This characteristic was common to the patterns for frequencies below 5–6 GHz. This phenomenon indicates that radio waves propagate easily in the region with pedestrians.

The level of the orthogonal polarization is much lower (about 20 dB) than that of the same polarization. Preceding the measurement, we measured the cross-polarization discrimination for the antenna in an anechoic chamber, and the value was found to be about 20 dB. Hence, the mode conversion seems to be negligible, although there are many scatterers and obstacles in the street.

In order to confirm what distribution a mode propagates, we measured the field distributions in the transverse cross section at a distance of 50 m from the transmitting antenna. The field distributions measured at a frequency of 500 MHz are shown in Figs. 3 and 4, together with theoretical patterns to be discussed in the next section. The receiving antenna was moved horizontally at intervals of 45 cm and was kept at a constant height of 1 m from the floor (Fig. 3), while the receiving antenna was moved vertically at intervals of 50 cm above the centerline of the floor (Fig. 4). It is seen that the horizontal patterns in Fig. 3 are close to cosine distributions, and that the vertical patterns in Fig. 4 are close to deformed cosine distributions. Similar patterns are seen in other frequencies below 5–6 GHz. The most significant feature is that the maximum field strength occurs in the region with pedestrians for both polarized waves, as in Fig. 4. This phenomenon indicates that most of the energy travels in the region with pedestrians. Hence, this region might be considered a dielectric layer from an analytical point of view.

As this experiment was performed when there were many people walking over all regions, the received field strength varied with a temporal density of pedestrians. It took 1.5 h to carry out one measurement. If there were any differences in the density of pedestrians, the effect would result in a different attenuation constant. Hence, the attenuation slope is not unique, even in the same frequency. In addition to this fact, the value of the attenuation constant depends slightly on a selected interval because it is calculated from the received field strength by the least squares method. For these reasons, we repeated the same propagation test twice at different times in order to find out the range of the attenuation constant and to reduce errors in evaluating the value.

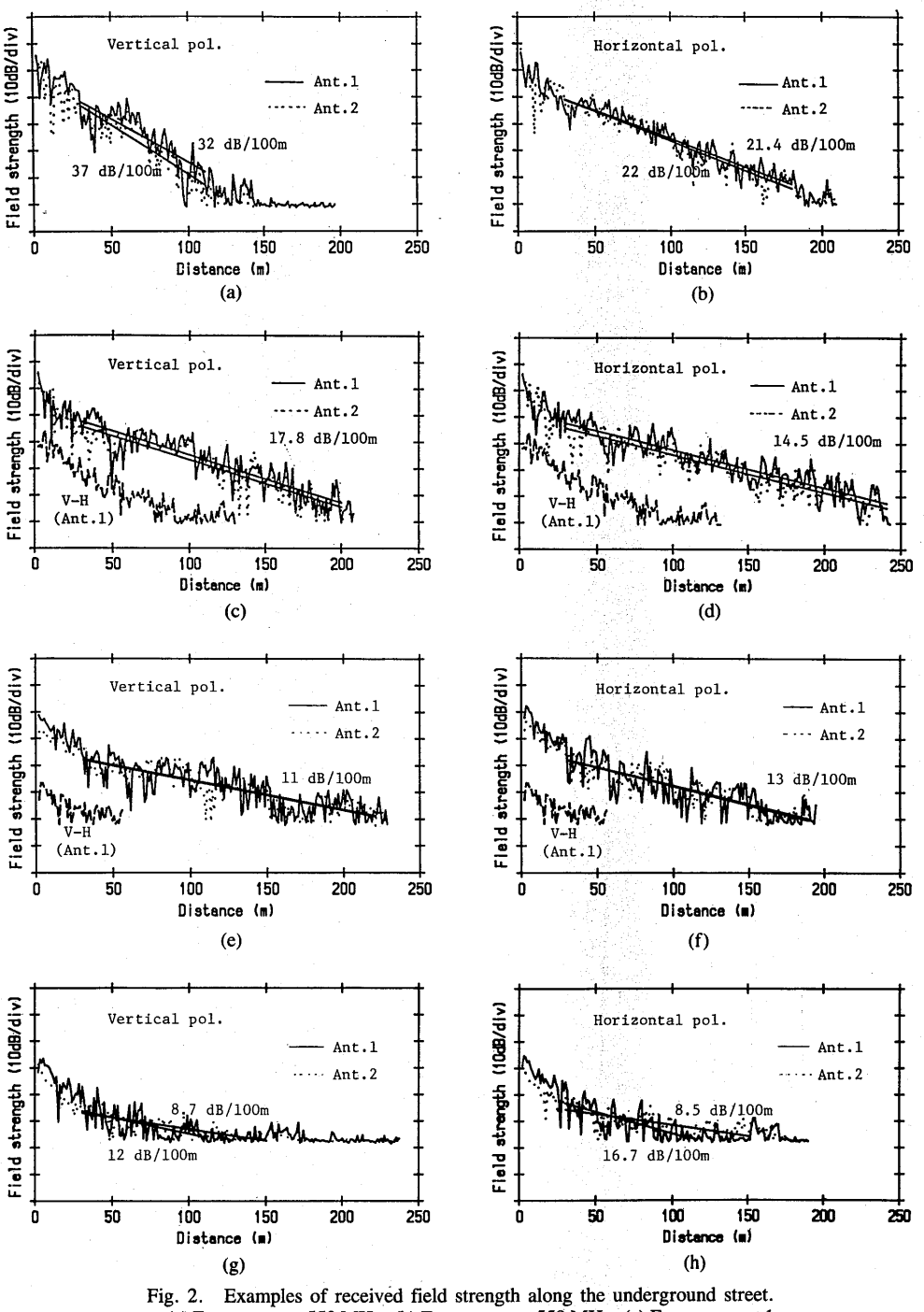

Fig. 2. Examples of received field strength along the underground street. (a) Frequency = 550 MHz. (b) Frequency = 550 MHz. (c) Frequency = 1 GHz. (d) Frequency = 1 GHz. (e) Frequency = 6.5 GHz. (f) Frequency = 6.5 GHz. (g) Frequency = 10 GHz. (h) Frequency = 10 GHz.

We calculated the experimental attenuation constant from the field strength received at different height, different measurement, and different selected intervals, except the near-field region (distances of which are within 20 m of the transmitter), in the same manner as [6]. This calculation has been repeated for all frequencies.

The calculated attenuation constants are shown in Fig. 5 as a function of frequency, with theoretical values to be discussed in the next section. As seen in this figure, the attenuation constant seems to decrease with increasing frequency as a whole. As a general tendency, the values and the frequency characteristics for both polarized waves agree with each other at higher frequencies above 2 GHz, although the propagation environment is so complex. On the other hand, the attenuation constants by Antenna 1 in upper free space are very close to those by Antenna 2 in the lower position below 5–6 GHz, and are larger than those by Antenna 2 above 6–7 GHz. This means that the region with pedestrians acts as a lossy dielectric component of rectangular waveguide below 5–6 GHz, and acts as highly lossy obstacles for radio propagation above 6–7 GHz. The absorption loss and/or the scattering loss by pedestrians has the dominant contribution to the propagation

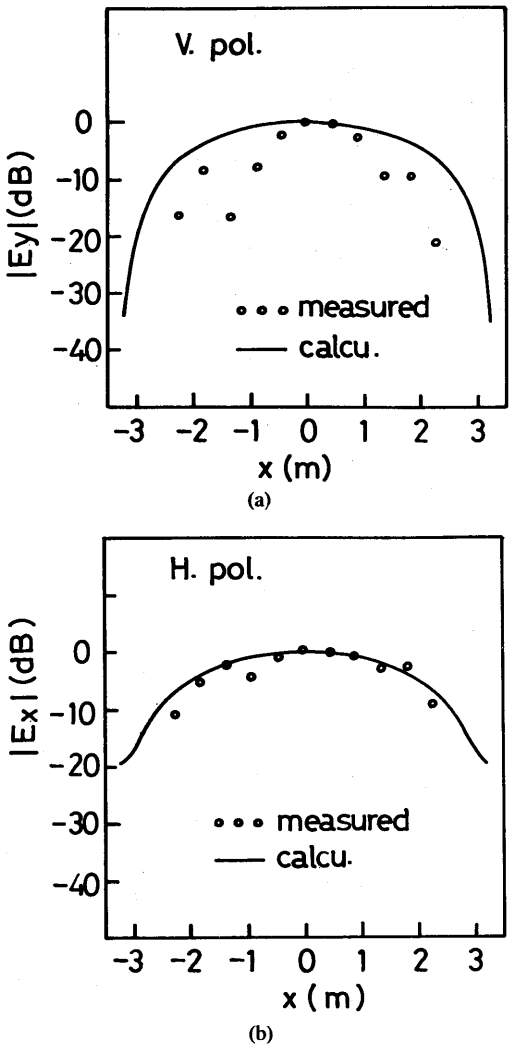

Fig. 3. Horizontal field distribution in the cross section of the underground street. (a) Vertical polarization. (b) Horizontal polarization.

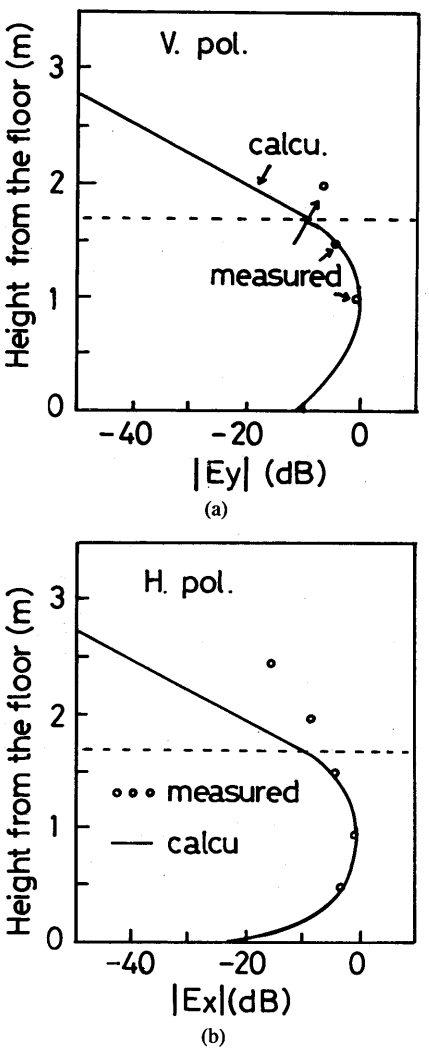

Fig. 4. Vertical field distribution in the cross section of the underground street. (a) Vertical polarization. (b) Horizontal polarization.

loss, since people become larger electrically and lossy in higher frequencies.

IV. Theoretical Consideration

It is difficult to obtain the exact propagation characteristics theoretically, considering boundary conditions for the structure. However, from the experimental field distribution in the cross section, the region with pedestrians might be considered or modeled as a dielectric layer from an analytical point of view. Hence, we assume the structure to be a partially loaded lossy dielectric waveguide, as shown in Fig. 6. Irregularly sized projections, such as signboards, lighting fixtures, and pillars on the ceiling and on sidewalls, are neglected to simplify the theoretical considerations.

A rigorous solution of Maxwell's equations for the simplified model in Fig. 6 would also be exceedingly complex; thus, we employed the method of effective dielectric constant [9]. The field components in the rectangular waveguide can be written in terms of two scalar potentials ϕ^e and ϕ^h:

$$E_x=\frac{1}{\epsilon_r(y)}\frac{\partial^2\phi^e}{\partial y\partial x}+\omega\mu k_z\phi^h \tag{1}$$

$$E_y=\frac{1}{\epsilon_r(y)}\left(k_z^2-\frac{\partial^2}{\partial x^2}\right)\phi^e \tag{2}$$

$$E_z=\frac{-jk_z}{\epsilon_r(y)}\frac{\partial\phi^e}{\partial y}-j\omega\mu\frac{\partial\phi^h}{\partial x} \tag{3}$$

$$H_x=-\omega\epsilon k_z\phi^e+\frac{\partial^2\phi^h}{\partial y\partial x} \tag{4}$$

$$H_y=\left(k_z^2-\frac{\partial^2}{\partial x^2}\right)\phi^h \tag{5}$$

$$H_z=j\omega\epsilon\frac{\partial\phi^e}{\partial x}-jk_z\frac{\partial\phi^h}{\partial y} \tag{6}$$

where ϵ and μ are the permittivity and permeability of free space, $\epsilon_r(y)$ is a relative dielectric constant in the region of application, and k_z is the propagation constant in the z direction.

As seen in (1)–(6), ϕ^e has the dominant contribution to the vertically polarized mode, which has the electric field predominantly in the y direction, and ϕ^h has the dominant contribution

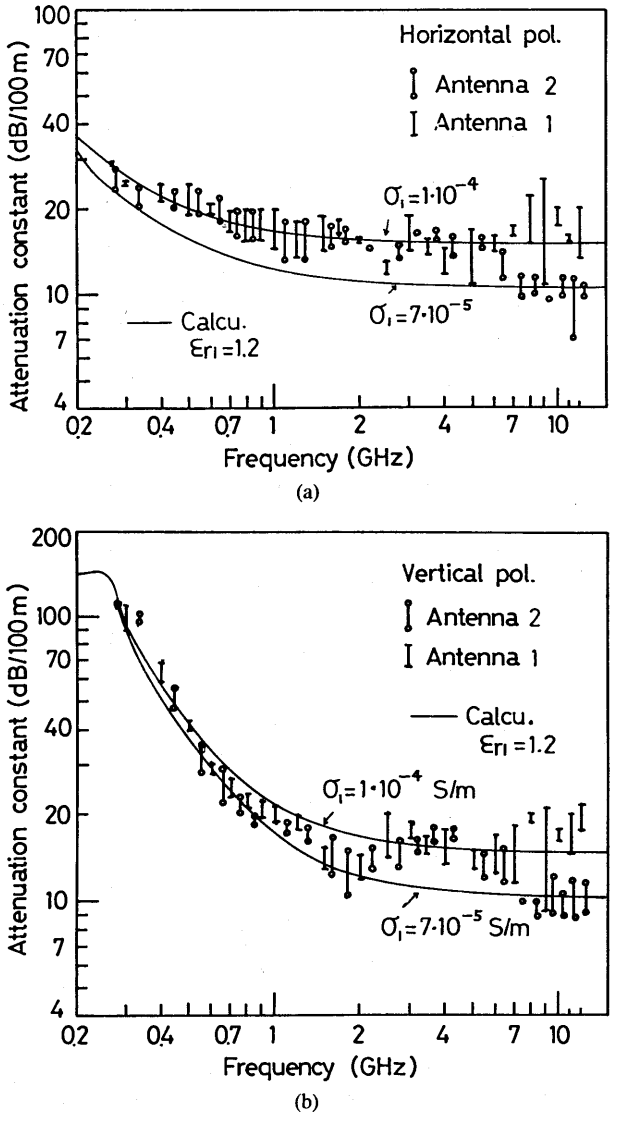

Fig. 5. Frequency characteristics of the attenuation constant in the underground street crowded with pedestrians. (a) Vertical polarization. (b) Horizontal polarization.

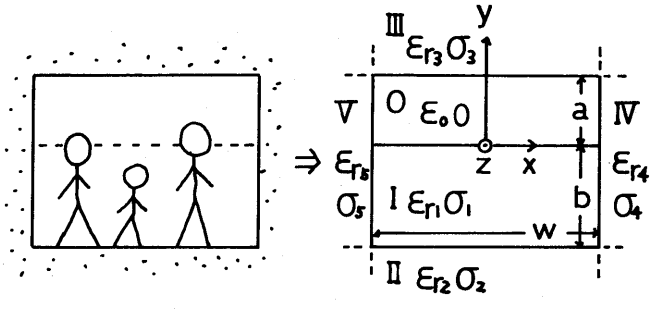

Fig. 6. A modeling of underground street crowded with pedestrians.

to the horizontally polarized mode, which has the electric field predominantly in the x direction. These modes correspond to the dominant modes in hollow tunnels or underground streets [1], [6] according to polarizations.

Under the condition that the transverse dimensions of a guide are somewhat larger than the free-space wavelength, a partially filled rectangular waveguide may be modeled as a combination of two parallel-plate guides, perpendicular to each other. This modification enables us to calculate the propagation constant in a rectangular waveguide easily. First, we decompose the rectangular guide into a horizontal parallel-plate guide, as shown in Fig. 7. The region with pedestrians is considered a homogeneous dielectric layer with relative dielectric constant ϵ_{r1} and conductivity σ_1. The other intrinsic constants and the coordinate system are defined in this figure.

For a vertically polarized wave, the field in each region can be represented as follows:

III $(y>a)$

$$\phi^e(y)=A\exp(-jk_{3y}y) \tag{7}$$

O $(a>y>0)$

$$\phi^e(y)=B\cos(k_{0y}y)+C\sin(k_{0y}y) \tag{8}$$

I $(0>y>-b)$

$$\phi^e(y)=D\cos(k_{1y}y)+F\sin(k_{1y}y) \tag{9}$$

II $(-b>y)$

$$\phi^e(y)=G\exp(jk_{2y}y) \tag{10}$$

where A, B, C, D, F, G are unknown amplitude coefficients, and k_{iy} $(i=0, 1, 2, 3)$ is the wavenumber in the y direction in the respective region and subject to the relation

$$k_{pz}^2=\epsilon_{ri}^*k_0^2-k_{iy}^2=\epsilon_0k_0^2-k_{0y}^2 \tag{11}$$

$$\epsilon_{ri}^*=\epsilon_{ri}-j(60\sigma_i\lambda) \tag{12}$$

$$i=1, 2, 3, \qquad k_0=2\pi/\lambda$$

where ϵ_{ri} is the relative dielectric constant (ϵ_0 is unity in the region O), σ_i is the conductivity, and λ is the free-space wavelength.

The tangential fields to the boundary are the H_x and the E_z, which are proportional to ϕ^e as

$$H_x\sim\phi^e$$

$$E_z\sim\frac{1}{\epsilon_r(y)}\frac{\partial\phi^e}{\partial y}.$$

By matching these components at boundaries $y=a$, 0, and $-b$, the characteristic equation for k_{1y} is given as follows:

$$\left[\frac{p}{\epsilon_{r1}^*}\tan p-j\frac{k_{2y}b}{\epsilon_{r2}^*}\right]\left[1+jk_{3y}a\frac{\epsilon_0}{\epsilon_{r3}^*}\frac{\tan q}{q}\right]\frac{a}{b}+\left[\frac{q}{\epsilon_0}\tan q-j\frac{k_{3y}a}{\epsilon_{r3}^*}\right]\left[1+jk_{2y}b\frac{\epsilon_{r1}^*}{\epsilon_{r2}^*}\frac{\tan p}{p}\right]=0 \tag{13}$$

where

$$p=k_{1y}b$$

$$q=k_{0y}a.$$

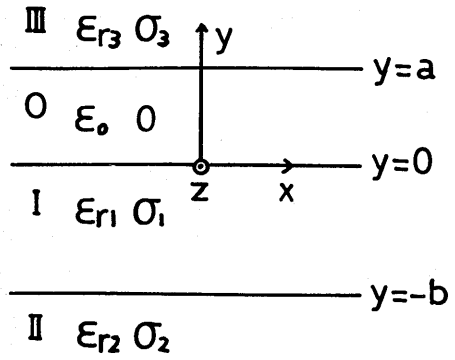

Fig. 7. Lossy dielectric parallel-plate waveguide.

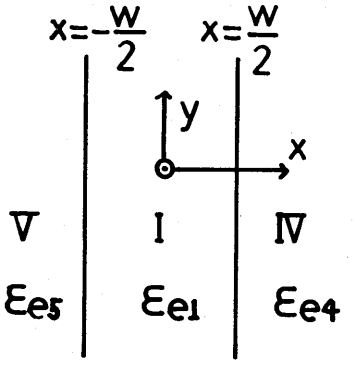

Fig. 8. Lossy dielectric guide structure using concept of effective dielectric constant.

The lowest value of k_{1y} will produce the fundamental mode for the structure; hence, we can calculate the field distribution in the y direction based on the k_{1y}.

Now, (11) may be rewritten in the following form:

$$k_{pz}^2 = \epsilon_{e1} k_0^2 \tag{14}$$

where

$$\epsilon_{e1} = \epsilon_{r1}^* - k_{1y}^2/k_z^2. \tag{15}$$

The term ϵ_{e1}, defined in (15), is the effective dielectric constant [9], and may be interpreted as that of a hypothetical medium in which the propagation constant is identical to that of the original structure.

In a similar manner, we can derive the effective dielectric constants in regions IV and V in Fig. 8. However, since most of the energy will travel in the inside region ($-w/2 < x < w/2$), we approximate the effective dielectric constant as follows:

$$\epsilon_{e4} = \epsilon_{r4}^*$$
$$\epsilon_{e5} = \epsilon_{r5}^*. \tag{16}$$

Next, we analyze the three-layered vertical-parallel structure shown in Fig. 8, having determined the effective dielectric constants ϵ_{e1}, ϵ_{e4}, ϵ_{e5}. Since the slabs are infinite in the y direction, there is only an x variation in the field. The field can be represented as follows:

IV ($x > w/2$)

$$\phi^e(x) = A_1 \exp(-j\xi x) \tag{17}$$

I ($w/2 > x > -w/2$)

$$\phi^e(x) = B_1 \cos(k_x x) + C_1 \sin(k_x x) \tag{18}$$

V ($x < -w/2$)

$$\phi^e(x) = D_1 \exp(j\eta x) \tag{19}$$

where A_1, B_1, C_1, D_1 are unknown amplitude coefficients, ξ and η are the wavenumbers in the x direction in regions IV and V, respectively. Here k_x is the wavenumber in region I subject to the relation

$$k_z^2 = \epsilon_{e1} k_0^2 - k_x^2 = \epsilon_{e4} k_0^2 - \xi^2 = \epsilon_{e5} k_0^2 - \eta^2 \tag{20}$$

where k_z is the propagation constant in the z direction and is identical with the propagation constant in the partially filled rectangular waveguide in Fig. 6.

By matching the tangential components E_y and H_z at boundaries at $x = w/2$ and $-w/2$, the characteristic equation for k_x can be derived as follows:

$$\left[u \tan u - j\frac{\eta w}{2}\right]\left[u + j\frac{\xi w}{2}\tan u\right] + \left[u \tan u - j\frac{\xi w}{2}\right]\left[u + j\frac{\eta w}{2}\tan u\right] = 0 \tag{21}$$

where

$$u = k_x w/2.$$

Similarly, the characteristic equations for the horizontally polarized mode can be obtained:

$$[p \tan p - jk_{2y}b]\left[1 + jk_{3y}a\frac{\tan q}{q}\right]\frac{a}{b} + [q \tan q - jk_{3y}a]\left[1 + jk_{2y}b\frac{\tan p}{p}\right] = 0 \tag{22}$$

$$\left[u \tan u - j\frac{\epsilon_{e1}^*}{\epsilon_{e4}^*}\frac{\xi w}{2}\right]\left[u + j\frac{\epsilon_{e1}^*}{\epsilon_{e5}^*}\frac{\eta w}{2}\tan u\right] + \left[u \tan u - j\frac{\epsilon_{e1}^*}{\epsilon_{e5}^*}\frac{\eta w}{2}\right]\left[u + j\frac{\epsilon_{e1}^*}{\epsilon_{e4}^*}\frac{\xi w}{2}\tan u\right] = 0 \tag{23}$$

where

$$p = k_{1y}b$$
$$q = k_{0y}a$$
$$u = k_x w/2.$$

V. Comparison with the Experimental Results

The characteristic equations (13) and (21)–(23) are solved numerically, and the results for the field distribution are shown in Figs. 3 and 4. As is evident from these figures, the calculated results characterize the experimental pattern well, especially in the region with pedestrians.

The parameters chosen in the calculation are

$$a=1.3\text{ m}, \quad b=1.7\text{ m}, \quad w=6.4\text{ m}$$

$$\epsilon_{r1}=1.2, \quad \sigma_1=10^{-4}\ \text{S/m}$$

$$\epsilon_{ri}=5, \quad \sigma_i=0.1 \quad (i=2, 3, 4, 5).$$

The values of intrinsic constants in the surrounding mediums are the representative values in the microwave frequency band, and the variation of these parameters produced little change in the theoretical curve except in the VHF band. On the other hand, since the intrinsic constants in the region with pedestrians are unknown, we calculated the curve with appropriate parameters. Increasing the relative dielectric constant ϵ_{r1} produced a discrepancy between the theoretical curve and the experimental data. The smaller value of ϵ_{r1} produced closer agreement. In addition, from the fact that there are 2–3 persons/10 m in the street, the region with pedestrians is considered as a sparse dielectric medium consisting of air and pedestrians. Hence, the value of ϵ_{r1} was chosen to be 1.2–1.3 to agree with the experimental results. The conductivity σ_1 from 0 to 10^{-3} S/m, gave similar patterns.

The theoretical attenuation constants are shown in Fig. 5 as a function of frequency, based on the above-mentioned parameters as well as on a parameter $\sigma_1 = 7\cdot10^{-5}$. The value of the attenuation constant is sensitive to the conductivity σ_1, as seen in Fig. 5, and less sensitive to the intrinsic constants in the surrounding mediums and ϵ_{r1}, although these results are not presented in graphical form in this paper. Hence, the conductivity has the dominant contribution to the attenuation constant. The theoretical curves characterize the experimental results well for both polarized waves.

From Figs. 3–5, the theory is applicable to determine the propagation characteristics in the underground street crowded with pedestrians to a certain degree of approximation. The effect of pedestrians on the attenuation constant can be determined mainly by the factor σ_1. Hence, the dependency of the attenuation constant on the traffic density of pedestrians might be treated by a function of σ_1, from the theoretical point of view.

VI. Conclusion

We measured the propagation characteristics of radio waves in an underground street crowded with pedestrians and derived the attenuation constant from 250 MHz to 12.4 GHz. From the experimental results, the attenuation constant decreases with increasing frequency as a whole. In the analytical formulation, the structure is modeled as a partially filled rectangular waveguide. Based on the method of effective dielectric constant, we calculated the field distribution and the attenuation constant, which were in close agreement with the experimental data below 5–6 GHz. This method is an approximate approach; however, it is expected to work well for the problem of propagation characteristics in guides crowded with pedestrians or obstacles.

There still remains a problem of how to decide definitely the relative dielectric constant and the conductivity in the region with pedestrians. It is necessary to treat this problem in a future investigation.

Acknowledgment

The authors wish to thank Y. Yamamoto, Chief Director of the Checking Center against Disaster of Niigata Chikakaihatsu Co., Ltd., for his kind cooperation, and also the people working at his company.

References

[1] A. G. Emslie, R. L. Lagace, and P. F. Strong, "Theory of the propagation of UHF radio waves in coal mine tunnels," *IEEE Trans. Antennas Propagat.*, vol. AP-23, no. 2, pp. 192–205, Mar. 1975.

[2] J. Chiba, T. Inaba, Y. Kuwamoto, O. Banno, and R. Sato, "Radio communication in tunnels," *IEEE Trans. Microwave Theory Tech.*, vol. MTT-26, no. 6, pp. 439–443, June 1978.

[3] S. F. Mahmoud and J. R. Wait, "Geometrical optical approach for electromagnetic wave propagation in rectangular mine tunnels," *Radio Sci.*, vol. 9, no. 12, pp. 1147–1158, Dec. 1974.

[4] B. Jacard and O. Maldonado, "Microwave modeling of rectangular tunnels," *IEEE Trans. Microwave Theory Tech.*, vol. MTT-32, no. 6, pp. 576–581, June 1984.

[5] H. Kishimoto, "Indoor radio propagation analysis by ray method," IECE of Japan, Tech. Rep. on Antennas Propagat., A.P76-62, 1976.

[6] Y. Yamaguchi, T. Abe, and T. Sekiguchi, "Experimental study of radio propagation characteristics in an underground street and corridors," *IEEE Trans. Electromagn. Compat.*, vol. EMC-28, no. 3, pp. 148–155, Aug. 1986.

[7] S. Kozono, T. Suzuki, and T. Hanazawa, "Experimental study of mobile radio propagation characteristics in rectangular tunnels," *Trans. IECE of Japan,* vol. J62-B, no. 6, June 1979.

[8] J. Chiba and K. Sugiyama, "Effects of trains on cutoff frequency and field in rectangular tunnels as waveguide," *IEEE Trans. Microwave Theory Tech.*, vol. MTT-30, no. 5, pp. 757–759, May 1982.

[9] W. V. Mclevige, T. Itho, and R. Mittra, "New waveguide structure for millimeter-wave and optical integrated circuits," *IEEE Trans. Microwave Theory Tech.*, vol. MTT-23, no. 10, pp. 788–794, Oct. 1975.

[10] D. A. Hill, "Electromagnetic propagation in an asymmetrical coal seam," *IEEE Trans. Antennas Propagat.*, vol. AP-34, no. 2, pp. 244–247, Feb. 1986.

[11] A. G. Emslie and R. L. Lagace, "Propagation of low and medium frequency radio waves in a coal seam," *Radio Sci.*, vol. 11, pp. 253–261, 1976.

[12] J. R. Wait, "Note on the theory of transmission of electromagnetic waves in a coal seam," *Radio Sci.*, vol. 11, pp. 263–265, 1976.

[13] J. R. Wait, *Electromagnetic Wave Theory.* New York: Harper and Row, 1985.

[14] Y. Yamaguchi, T. Abe, and T. Sekiguchi, "Improvement of attenuation characteristics in tunnels (I)," IECE of Japan, Tech. Rep. on Antennas Propagat., A.P83-11, May 1983.

[15] J. N. Murphy and H. E. Parkinson, "Underground mine communications," *Proc. IEEE,* vol. 66, no. 1, pp. 26–50, Jan. 1978.